Mathematical Biosciences and Engineering

MBE, 17(3): 2218–2235.
DOI: 10.3934/mbe.2020118
Received: 02 August 2019
Accepted: 04 November 2019
Published: 14 January 2020

http://www.aimspress.com/journal/MBE

Research article

The basics of a system for evaluation of fiber-cement materials based on acoustic emission and time-frequency analysis

Anna Adamczak Bugno*and Aleksandra Krampikowska

Faculty of Civil Engineering and Architecture, Kielce University of Technology, Aleja Tysiąclecia Państwa Polskiego 7, 25-314 Kielce, Poland

*** Correspondence:** Email: aadamczak@tu.kielce.pl.

Abstract: Fiber-cement building products are increasingly used in construction. They are used as building and finishing material for facades, internal walls and roofs. Numerous advantages such as relatively low weight, low absorbability and relatively high strength allow to use these materials in bulky constructions and in buildings which are commonly considered tall. Safety reasons, however, point to the need to control the condition of materials used to erect such structures. It is also in line with the more and more widely implemented concept of monitoring the state of the structure and its components over their entire period of use (SHM). The article presents the results of experimental tests on flexural strength of cement-fiber boards in an air-dry state, which have been soaked in water for 24 hours and subjected to high temperature. The paper also presents a possibility to use a non-invasive method of acoustic emission and wavelet analysis for testing cement boards reinforced with cellulose fibers. Obtained results allow to track the change of mechanical parameters in boards subjected to environmental and exceptional factors. These results also confirm the applicability of the presented methods as instruments for observing the condition of the panels used.

Keywords: cement-fibre boards; nondestructive methods; wavelet analysis; mechanical parameters

1. Introduction

Currently, fiber-cement boards are considered to be attractive and reliable facade cladding. In the 70's and 80's of the previous century, asbestos was used for the production of fiber and cement. No one realized at that time that in several dozen years it would have to be eliminated and removed from the roofs. Today, when we talk about fiber-cement, hardly anyone associates it with old

asbestos-cement boards, commonly referred to as Eternit. In the production process, asbestos has been replaced by other, completely harmless materials, and the appearance of fiber-cement in no way resembles those not too pleasant, wavy boards. The material is still gaining popularity and it is used both in single-family housing and in the construction of public facilities. It is now widely known as a roofing material, but also more and more frequently used on building facades [1–5].

The fiber-cement is made of Portland cement and synthetic cellulose fibers. Cement accounts for 90% of the production mix and is necessary for the proper binding of the material and its ultimate durability. Cellulose make up for 10% of the fiber-cement. It is a gap filler and an additive that provides the appropriate volume of the liquid in the binding stage [6]. It also increases the density of the product. To improve the appearance and flexibility of fiber-cement boards chalk is added to the mixture. The technology of production of fiber-cement materials consists in overlapping successive thin layers of the mixture, which are strongly pressed together before the process of slow curing. The result is very high strength of the fiber-cement [7–9].

Cement-fiber boards are building materials intended mainly for light and ventilated facades, both in single-family houses and large-size public utility buildings. Fiber-cement boards can also be used for finishing attics, window elements, eaves and balconies. The material is recommended for use not only in newly-built facilities, but also in the process of renovation of existing buildings.

Fiber-cement elements are characterized by a resistance to moisture and a very high pH level, which ensures protection against mold growth. The robust construction of the building board means that they also demonstrate very high mechanical strength and maintain their original shape despite changing weather conditions. It is also worth noting that the boards provide very good acoustic insulation. Moreover, the layer of fiber-cement boards greatly improves the energy properties of the building, which is why they are willingly used in passive construction.

The installation of fiber-cement boards consists in attaching them to an aluminum profile using special gouging, which ensures stability of the boards even during strong wind. Facade panels can be delivered cut to the right size, ready for installation, or can be cut at the construction site using standard building tools, according to the instructions given by the manufacturer.

In the literature of the subject one can find the results of a number of studies regarding both mechanical and physical properties as well as the microstructure of materials produced from fiber-cement. One can draw the following conclusions from them [10]:

- wood pulp, cellulose fibers and sisal threads are the most commonly used form of fibers for the preparation of cement-fiber composites [11–13];
- to obtain cement-fiber elements of the required mechanical strength, it is necessary to properly distribute the fibers in the matrix. This fact is conditioned by the production methods, which mainly consist of varieties of the traditional Hatscheck method [14,15];
- due to the fact that cement-fiber composites are produced as thin panels of large surfaces, the most recommended method of mechanical testing is bending in a beam-supported pattern in 3 or 4 points;
- various processing methods can be used to improve the durability of cement-cellulosic composites: Using pozzolanic additives (directly incorporated into the cement mass or applied to fibers) and/or curing in a CO_2 atmosphere.

In the research of cementitious materials reinforced with cellulose fibers, acoustic methods (ultrasonic, acoustic emission) are also used [16–23]. Observations have also been made with the use of X-ray microtomography [24,25].

Because of a wide use of fiber-cement materials in construction, including the construction of large-size and high-rise buildings, it is considered appropriate to find a method that will allow to control and monitor these elements in the real state. This is justified, first of all, by security reasons and the broadly understood subject of monitoring a construction throughout its existence (SHM) [26–38].

2. Materials and methods

2.1. Materials

The studies have been carried out on three types of fiber-cement materials marked with the letters BD, BS and BB. The elements for testing were cut from a cement-fiber board of 3.1 × 1.25 m. The dimensions of the elements tested were 300 × 50 × 8 mm. Each series consisted of 5 samples. The boards marked with symbols BD were in a natural state [6]. The BS designation indicates that the boards were subjected to water for 24 hours immediately before the test, while BB samples were placed in a laboratory furnace for 3 hours and fired at 230 ℃.

The boards consist of the following components:

- Portland cement,
- mineral binders,
- organic reinforcing fibers (about 6%),
- admixtures.

The boards are traditionally produced using a Hatschek machine, compressed and air dried [1,6,16,22].

Technical data of tested boards is presented in Table 1.

Table 1. Technical data of the tested board.

Parameter	Conditions	Standard	Value	Unit
Density	Dry condition	EN 12467	> 1,65	g/cm^3
Flexural strength	Perpendicular	EN 12467	24,0	N/mm^2
	Parallel	EN 12467	18,5	N/mm^2
Modulus of elasticity		EN 12467	12 000	N/mm^2
Stretching at humidity	30–95%		1,0	mm/m
Porosity	0–100%		> 18	%

Bending tests were carried out in a free-supported beam scheme loaded with concentrated force in the middle of the span (Figure 1). The loading speed was 0.1 mm/min. Using the Vallen software, the acoustic emission (AE) parameters were recorded during the tests.

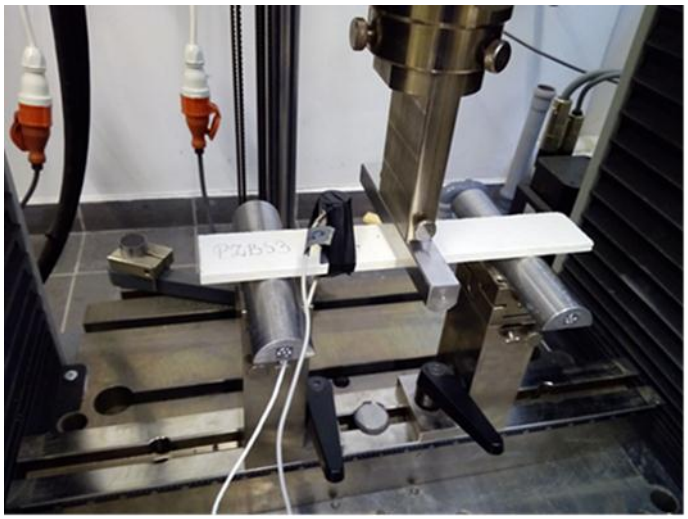

Figure 1. Test stand with a test sample.

2.2. Methods

The main task of the measurement system is to detect, record, filter and analyze signals generated by AE sources. The basic measurement system of the acoustic emission method to assess the condition of fiber-cement elements consists of sensors, preamplifiers, and a recording processor along with analyzing programs [24,39,40]. The diagram of the AE measurement system is shown in Figure 2.

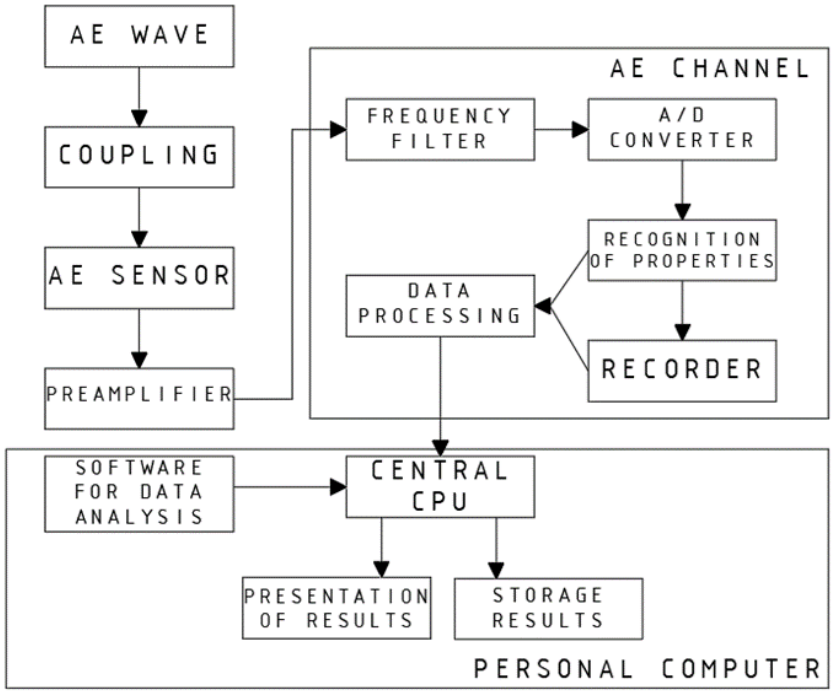

Figure 2. Diagram of the AE measuring system.

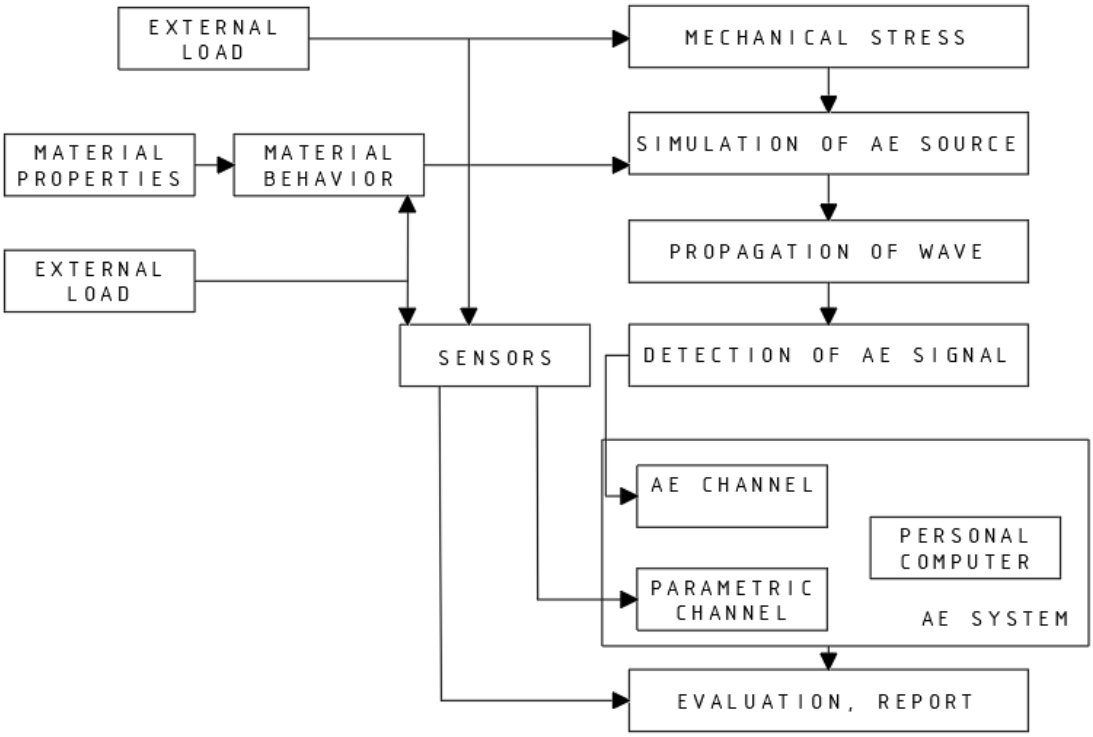

Figure 3. AE process chain.

During the analysis of individual stages of the measurement (Figures 2 and 3), the waves generated by the damage are recorded by means of acoustic emission sensors—converters changing the elastic wave into an electrical signal. There is a whole range of sensors that differ in their size and purpose, fixed to the tested surfaces using magnetic, glued or other holders, which guarantee the adhesion of sensors to the tested structure.

For the testing of cement-fiber boards, broadband sensors with a measuring range of 30–450 kHz are used [41–43].

Not a less important element that guarantees the correctness of the measurement is good coupling of the sensor with the tested surface. This is achieved by lubricating the surface and sensor to be tested, e.g. with silicone grease, technical vaseline or other coupling agent.

In the case of cement-fiber boards, the AE signals generated by the damage are too weak to be detected, hence preamplifiers are used to amplify the signals recorded by the sensors before further processing. A typical amplification range varies from 40 to 60 dB [6,44].

The planned system for assessing the condition of the boards consists in arranging several sensors (Figure 4a) and the location of the wave source over the entire tested element by comparing the time of the arrival of the signals to the sensors using a technique of triangulation.

Signals recorded in this way will allow to locate the boards in which the generated descriptors reach the highest values (Figure 4b). In the next step, the tests will be carried out on these elements. During the tests, both typical parameters of AE signals will be analyzed (e.g. amplitude, signal energy, duration of signals) and frequencies in which they appear.

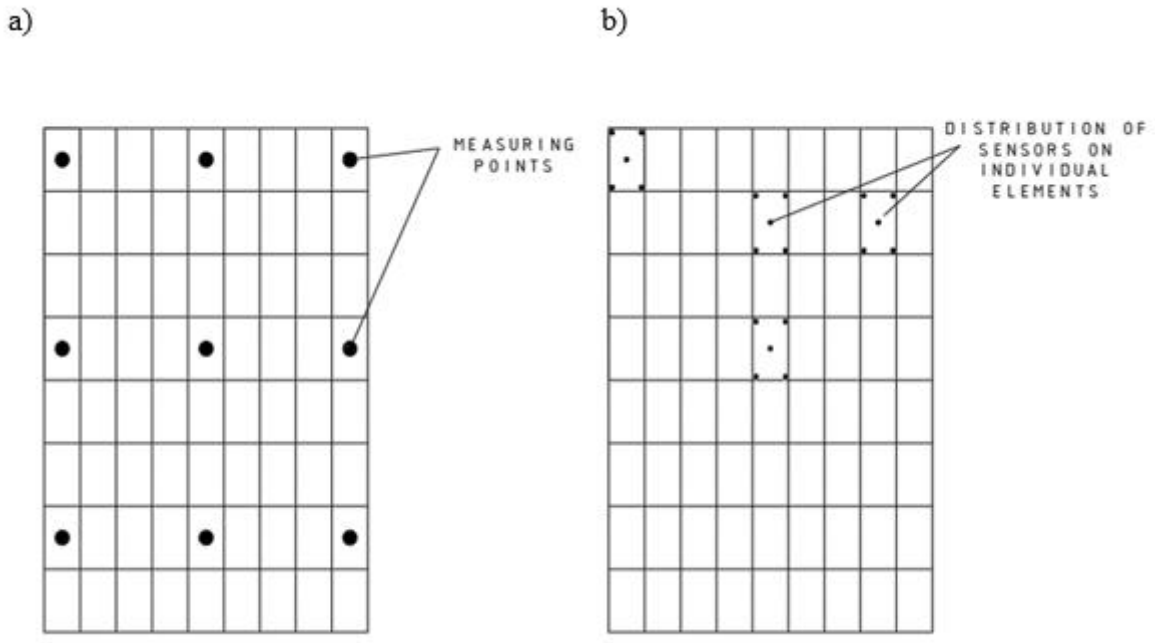

Figure 4. Scheme of the distribution of measuring points (a) on the entire tested element; (b) on individual boards.

The tests carried out so far in laboratory conditions, whose results are presented in the next item, confirm the applicability of the indicated method as the basis of the proposed system. In the near future, it is planned to transfer it to elements with real dimensions.

As a basic tool for data analysis in the Vallen programs examining the sound emission data, whose processor is used for the study in question, Fourier transform and wavelet analysis have been used.

A fast Fourier transform is a total transformation of time series consisting in the transition from the time domain to the frequency domain, which distributes a given time series into periodic functions in such a way that their convolution gives a primitive function. As a result of using FFT, we get information about the power of oscillation as a function of the period—we lose data when a given change occurred. The disadvantage of the Fourier transform is the fact that it is only suitable for studying stationary series [37,38].

A wavelet transform is a transformation similar to the Fourier transform, but it is ideal for studying non-stationary series. It is based on dividing the signal into smaller parts, and then comparing them with the scaled and shifted version of the basic wavelet. As a result of using a continuous wavelet transform, we obtain results on the time-scale plane, therefore an important issue when analyzing time series by this method is to recalculate the obtained scale to the corresponding frequency. The wavelet transform has become an alternative to the Fourier transform, because it does not lose the character of the tested series (it is suitable for analyzing non-stationary signals). In addition, it allows to compress images or denoise signals without any degradation.

The most characteristic feature of the wavelet transform is that individual wavelet functions are well located in time (or space—for images) and at the same time well describe the signal in the frequency domain, strictly speaking, the so-called scale. In addition, unlike the sine and cosine functions that define the unique Fourier transform, there is no single, unique set of wavelet base

functions. The wavelets differ in the compactness of the time location and the smoothness and softness of the shapes. The resulting ability of wavelets to describe signals with "discontinuities", with a limited number of coefficients and with location in time, determines its superiority over the Fourier transform.

It is believed that the tool, which is the wavelet analysis, will allow to trace the frequencies in which the mechanical parameters of the cement-fiber materials tested change.

3. Results and discussion

A number of registered AE parameters have been analyzed using the Vallen Visual AE program. The characteristics are shown in Tables 2–4.

Table 2. Characteristics of acoustic emission for BD series samples [45].

Sample designation	BD1	BD2	BD3	BD4	BD5	Arithmetic average	Standard deviation
Fmax [kN]	0.261	0.261	0.255	0.274	0.258	0.262	0.007
Maximum number of AE counts	306	526	572	462	394	452	105.660
Maximal energy of AE events [eu]	1494525	1094933	1260601	985412	1014256	1169945.4	210647.205

Table 3. Characteristics of acoustic emission for BS series samples.

Sample designation	BS1	BS2	BS3	BS4	BS5	Arithmetic average	Standard deviation
Fmax [kN]	0.267	0.283	0.212	0.255	0.225	0.248	0.029
Maximum number of AE counts	432	445	655	572	498	520.4	93.249
Maximal energy of AE events [eu]	1283850	1456454	15923489	1015486	1174162	4170688.2	5878157.856

Table 4. Characteristics of acoustic emission for BB series samples.

Sample designation	BB1	BB2	BB3	BB4	BB5	Arithmetic average	Standard deviation
Fmax [kN]	0.117	0.166	0.158	0.188	0.105	0.147	0.035
Maximum number of AE counts	105	127	96	86	112	105.2	15.611
Maximal energy of AE events [eu]	684918	688215	79880	446273	597416	499340.4	254211.850

Figures 5–7 show examples of energy records of events as a function of time and number of counts over time.

Analyzing these figures, one can observe differences in the processes of destruction of individual samples. The values of the descriptors achieved when reaching the maximum force value differ from each other. In the presented scale, the acoustic activity before reaching the maximum

force for dry samples and ones soaked in water is practically null.

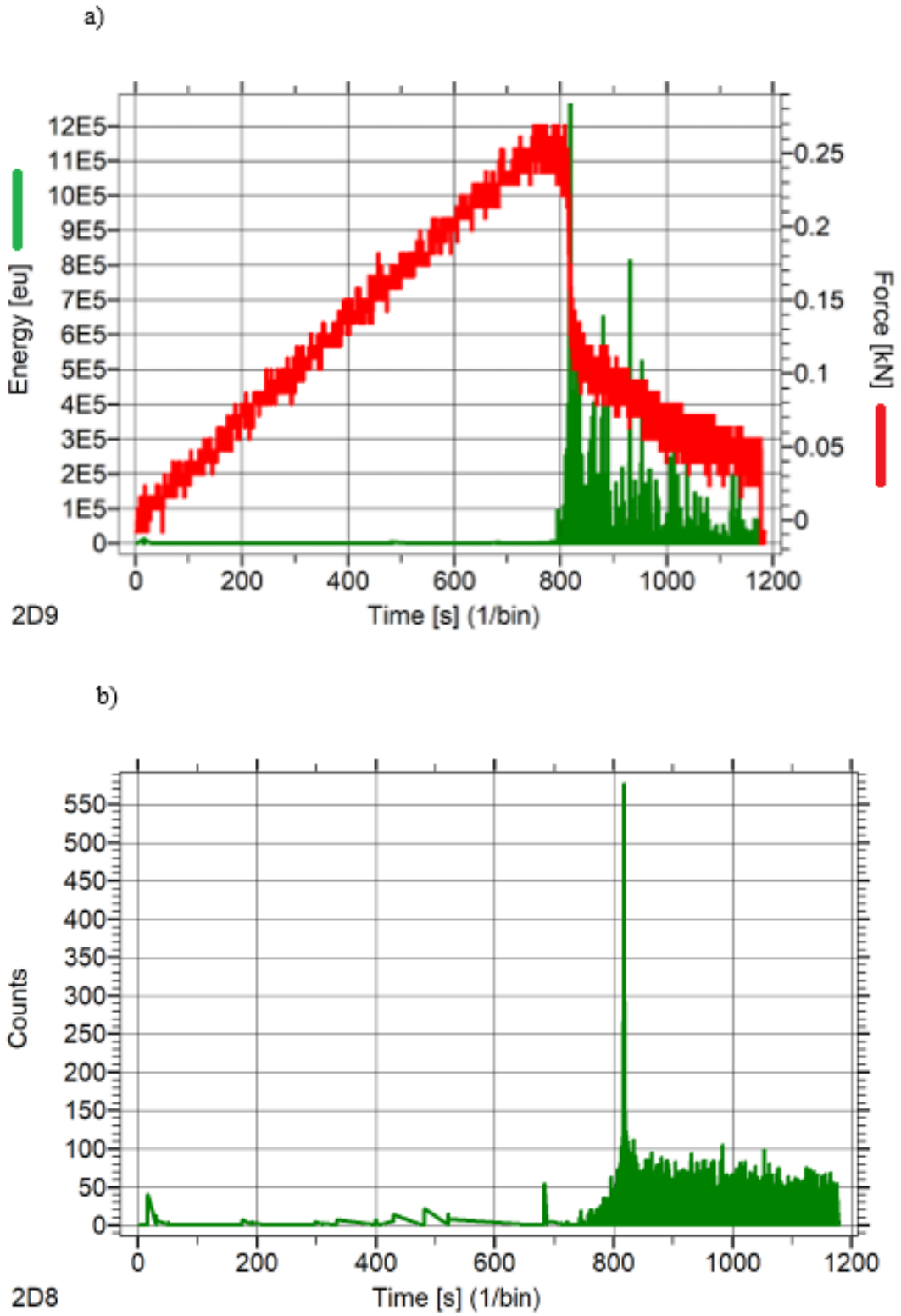

Figure 5. Graphical representation of registered AE parameters for one exemplary sample of the BD series (a) recording energy of signals in time with the load increase; (b) record of the number of counts over time.

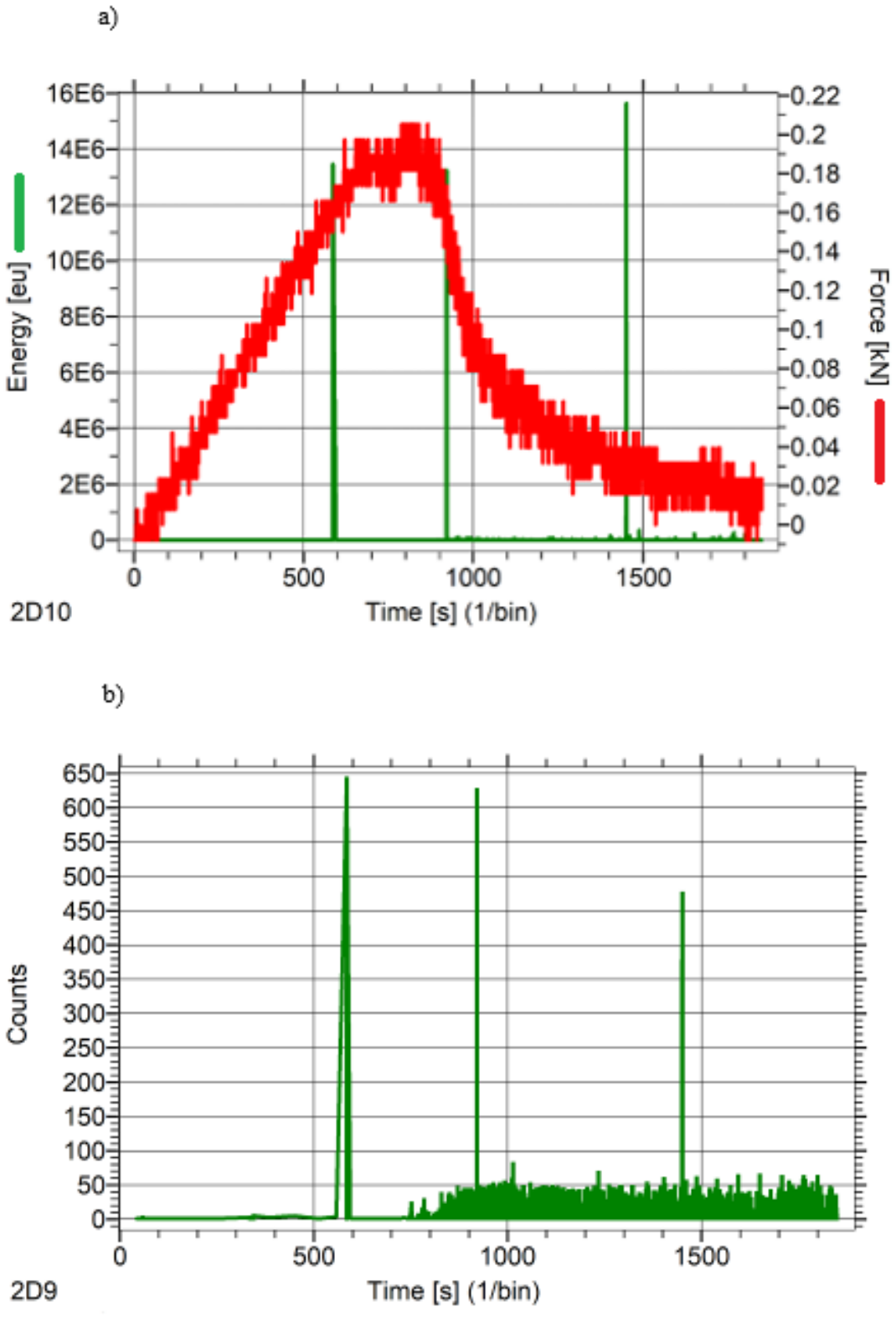

Figure 6. Graphical representation of registered AE parameters for one exemplary sample of the BS series (a) recording energy of signals in time with the load increase; (b) record of the number of counts over time.

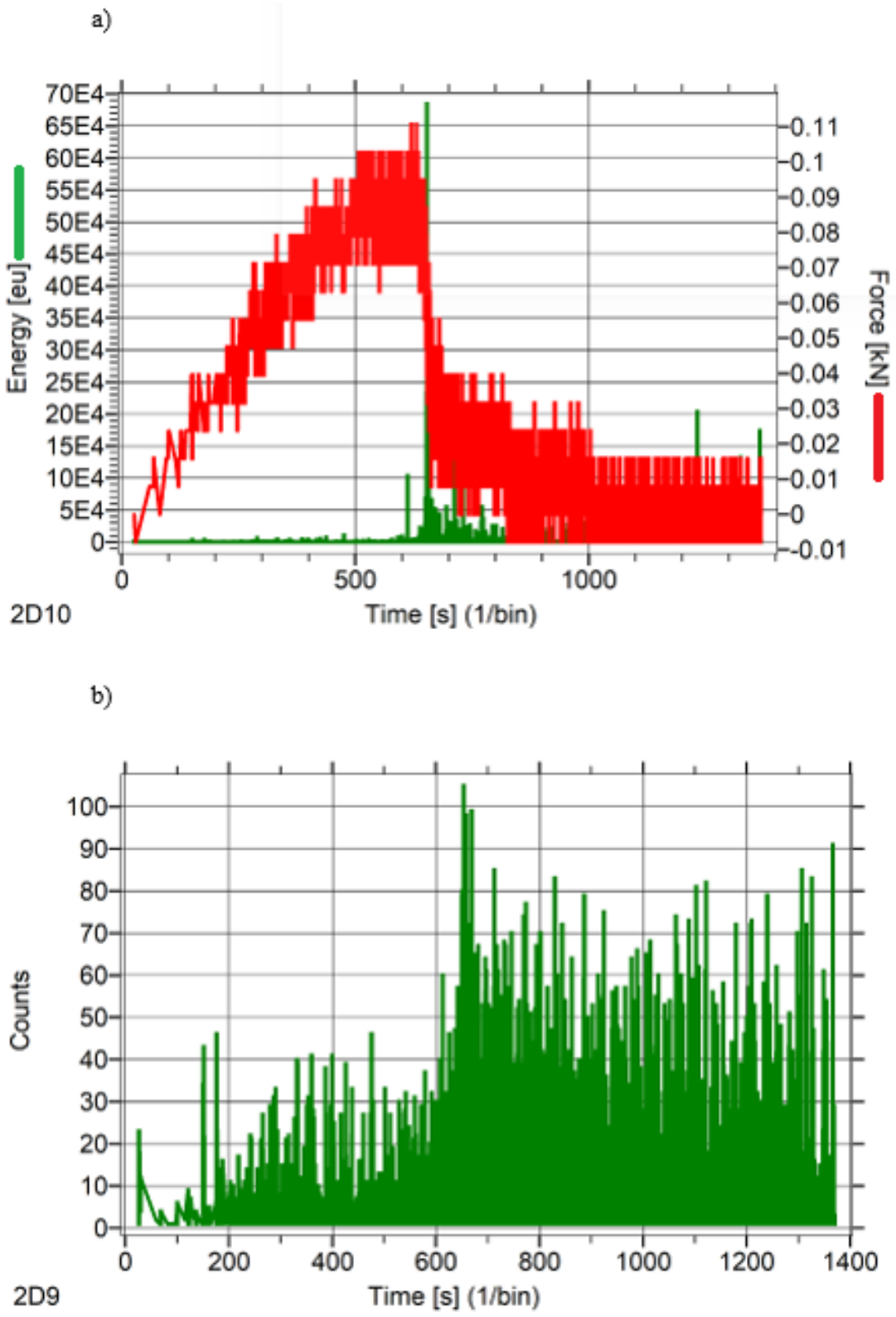

Figure 7. Graphical representation of registered AE parameters for one exemplary sample of the BB series (a) recording energy of signals in time with the load increase; (b) record of the number of counts over time.

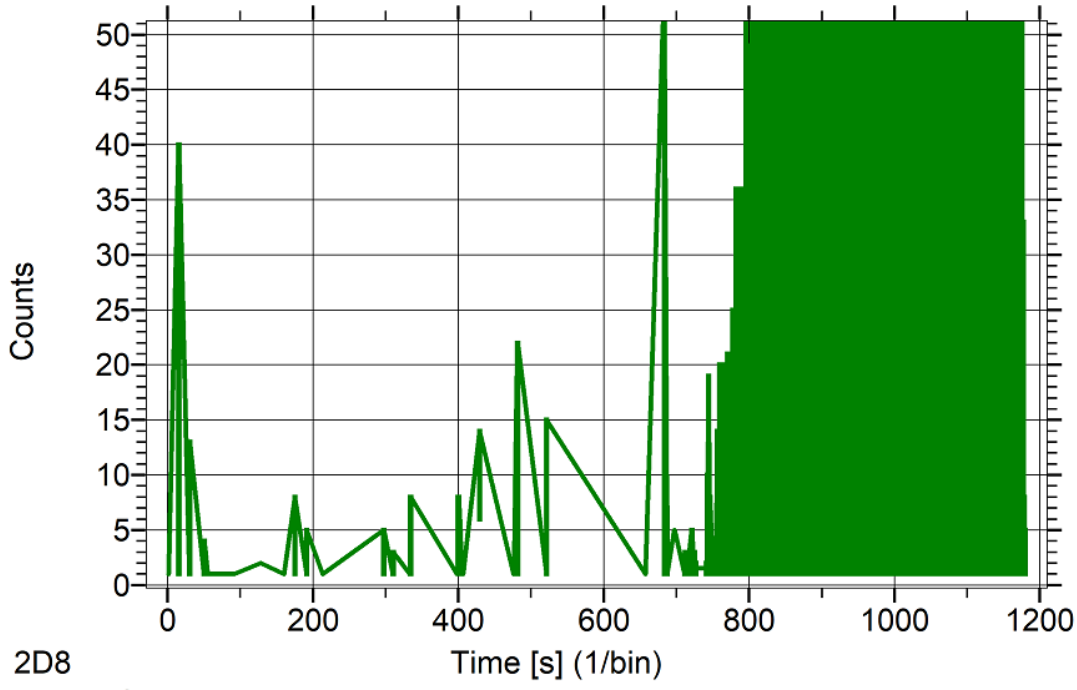

Figure 8. Scaled graph of the number of counts in time for an example sample of the BD series before reaching the maximum force value.

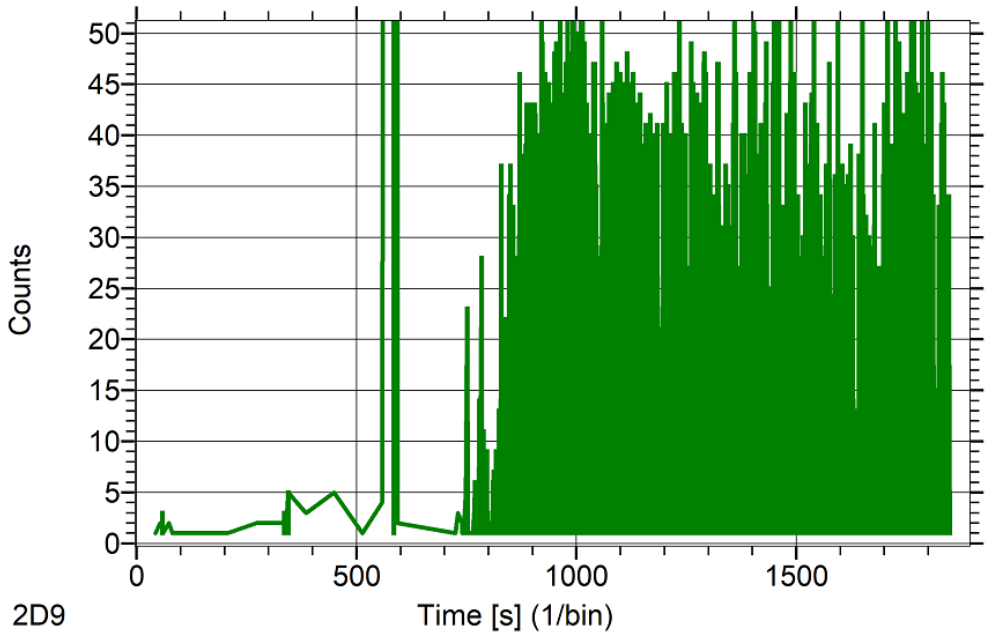

Figure 9. Scaled graph of the number of counts in time for an example sample of the BS series before reaching the maximum force value.

Only when the axis scale of the analyzed descriptor is increased before the moment of destruction (Figures 8 and 9) , differences can be seen. To this end, the graphs of the course of counts in time have been analyzed. It can be clearly observed that in the case of elements of the BD and BS

series, the counts achieved do not actually exceed a dozen or so before reaching the maximum strength level (only for the BD series). In addition, it can be stated that these values reach only a few events. Another situation has occurred in the case of the BB series sample—the majority of events before reaching Fmax exceed the number 20. The graph's course is dynamic throughout the analyzed period of time.

It is assumed that the microstructure of the tested elements has an impact on the nature of registered descriptors, which depends on the type of factors acting on the material. In the case of boards of the BD and BS series, the sample was destroyed due to exceeding the bending stress. In the analyzed waveforms, signals generated by pulling out fibers from the matrix and breaking the fibers can be observed. It is believed that a similar pattern of destruction of the analyzed samples of two series results from the fact that the material is resistant to water, and, therefore, the microstructures of both elements do not differ from each other.

In the case of the BB group, a high level of acoustic activity is observed before the moment of destruction. It is believed that this phenomenon is connected with fragile cracking of the matrix. When burned samples are destroyed, there is also a dramatic increase in registered descriptors. The material is destroyed due to exceeding the shear stress. The obtained results have been confirmed by microscopic observations [46]. It has been found that the fibers degraded as a result of high temperature.

However, the maximum value of the number of counts—on a similar level for elements from BD and BS series, is connected with the fact of breaking the reinforcement. Significantly lower level of counts at the moment of rupture for BB series boards is the result of gradual cracking of the matrix in the entire analyzed course up to the fragile fracture of the element.

Thanks to the conducted research, it has been possible to observe clear differences in the work of reinforced composites and the damaged fiber structure.

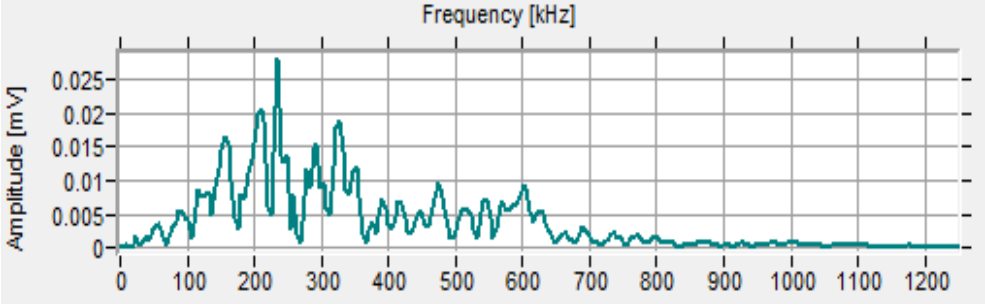

Figure 10. Graph of amplitude and frequency dependence for the sample signal from the BD series.

Using the Vallen Wavelet tool, which is a part of the Vallen AMSY-5 software, sample graphs of the frequency spectrum of the signal for the exemplary board BD series (Figure 10), BS (Figure 11) and the BB series (Figure 12) have been determined before the destruction [45]. Analyzing the presented graphs, one can observe that for the BD series sample the frequency range is between 0 and 700 kHz, and the peak amplitudes occur for frequencies in the range of 150–350 kHz. Analyzing the example chart for the element from the BS series, it is evident that the frequencies occurring are in the range of 0–700 kHz (although from 300 kHz their course reaches negligible amplitude values),

and the maximum amplitudes are achieved in the frequency range 50–150 kHz. In both cases, the entire frequency spectrum has been considered to be triggered by breaking the fibers. For the BB series sample, the frequency operation area is much narrower and amounts to 0–100 kHz. For the visible frequency range, the spectral characteristics are almost flat. It has been qualified as a form of events caused by fragile matrix cracking.

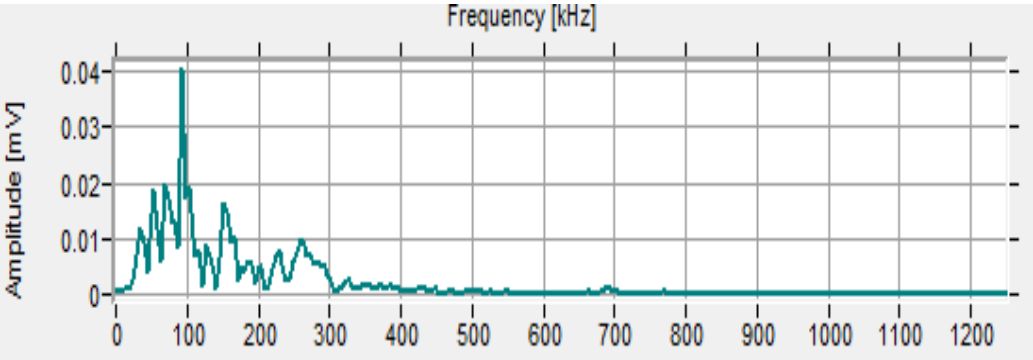

Figure 11. Graph of amplitude and frequency dependence for the sample signal from the BS series.

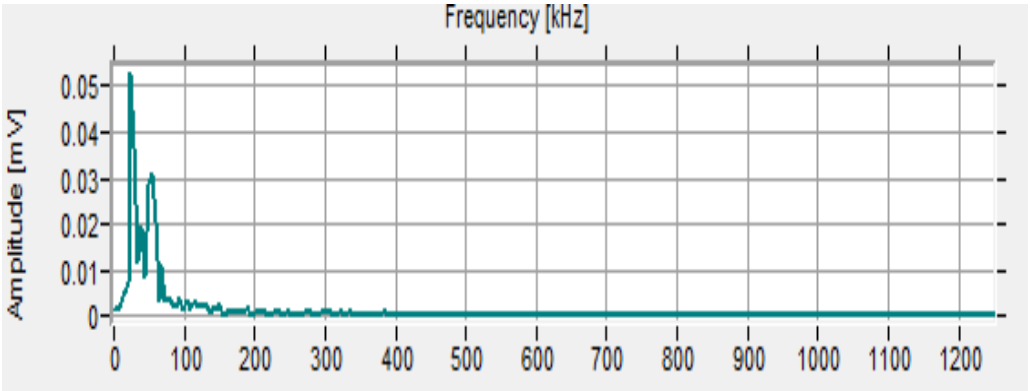

Figure 12. Graph of amplitude and frequency dependence for the sample signal from the BB series.

Using the aforementioned wavelet analysis module, spectrograms of the spectrum power density of the sample from the BD (Figure 13), BS (Figure 14) and the BB series (Figure 15) have also been determined. Analyzing the spectrograms, it is visible that in the case of the BD and BS series boards, the analyzed structures are distinguished by significant dynamics of the course over time. Clear delamination is also visible. Both of these properties have been related to cracking and plucking of reinforcement in the tested samples and gradual crack formation in the tensile zone of the analyzed elements.

For the samples from the BB series, the structures run evenly in the analyzed time. They also do not achieve significant frequency values. They have been associated with the gradual cracking of the fragile matrix of the samples.

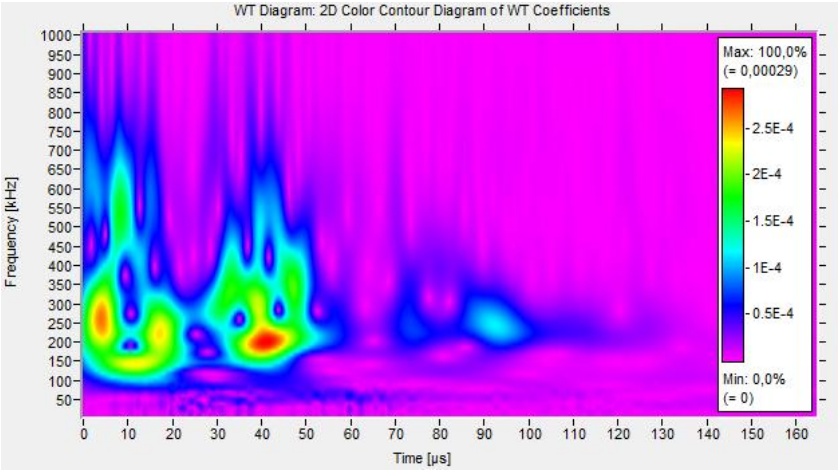

Figure 13. Power spectral density of AE signals generated during the bending of an exemplary sample of a series of BD.

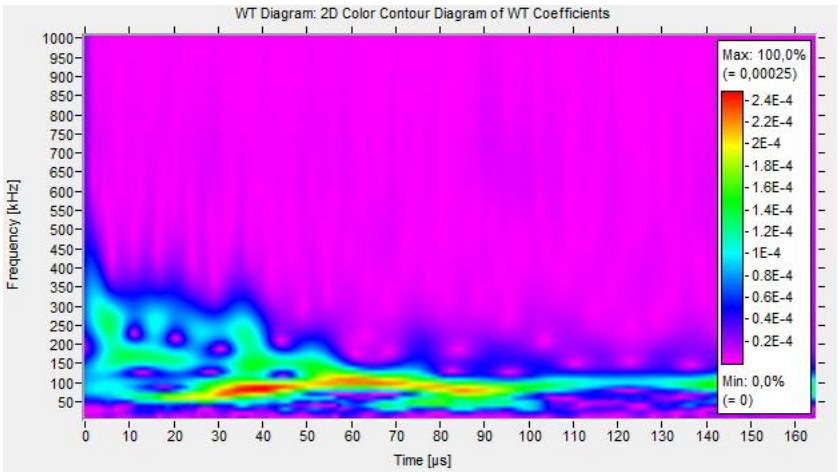

Figure 14. Power spectral density of AE signals generated during the bending of an exemplary sample of a series of BS.

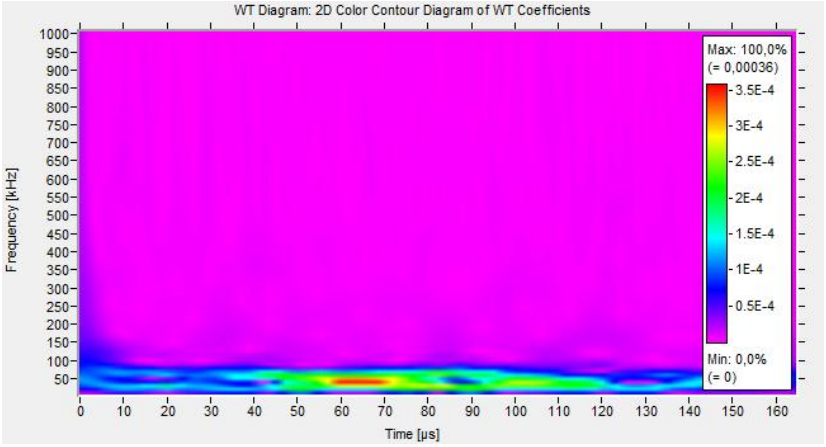

Figure 15. Power spectral density of AE signals generated during the bending of an exemplary sample of a series of BB.

4. Conclusion

A number of advantages of fiber-cement products accounts for the ever wider use of these materials in the production of new constructions and renovations of those already in use. A modern form and relative ease of assembly contribute to an increasing use of this material in projects of all types of buildings, both residential and public, including large-size and high-rise buildings. It should be noted, however, that one of the most important issues related to any construction project is construction safety. Ensuring this security requires, among other things, the control of a resulting object and its components during operation. It has been stated that an acoustic emission method may be an appropriate tool for such control of boards.

The article presents a proposal for applying the acoustic emission method based on the wavelet analysis as a tool for assessing the state of cement-fiber boards. The essentials of the system based on the indicated tools are also presented. The obtained results allowed to capture differences in the course of processes of destruction of materials with complete microstructure and with degraded fiber structure. Differences have been found in both the characteristics of registered AE parameters and frequency bands preceding the moment of sample destruction. The results presented differ in order of magnitude. It has been noted that the action of water does not significantly change the characteristics of AE. Clear differences have also been found in relation to the mechanical parameters of dry and fired samples—mainly the transmitted force, and the close relationship between them and the recorded descriptors has been confirmed. Therefore, it is believed that the presented system can be used to control the condition of fiber elements with a cement matrix, especially in cases of high temperatures caused by, for instance, fire or in the case of suspected degradation of fibers or manufacturing errors due to, for example, errors in the production process.The authors argue that the method of acoustic emission may prove particularly useful in the case of large-size pores in the structure of materials.

Conflict of interest

The authors declare no conflict of interest.

References

1. A. Akhavan, J. Catchmark, F. Rajabipour, Ductility enhancement of autoclaved cellulose fibre reinforced cement boards manufactured using a laboratory method simulating the Hatschek process, *Constr. Build. Mater.*, **135** (2017), 251–259.
2. P. J. Kim, H. C. Wu, Z. Lin, V. C. Li, B. deLhoneux, S. A. S. Akers, Micromechanics-based durability study of cellulose cement in flexure, *Cem. Concr. Res.*, **29** (1999), 201–208.
3. EN 12467—Fibre Cement Flat Sheets. Product Specification and Test Methods. Available from: https://infostore.saiglobal.com/en-us/Standards/EN-12467-2012-A2-2018-343722_SAIG_CEN_CEN_786757/.
4. G. H. D. Tonoli, S. F. Santos, H. Savastano, S. Delvasto, R. Mejía de Gutiérrez, M. D. M. Lopez de Murphy, Effects of natural weathering on microstructure and mineral composition of cementitious roofing tiles reinforced with fique fibre, *Cem. Concr. Compos.*, **33** (2011), 225–232.

5. K. G. Satyanarayana, G. G. C. Arizaga, F. Wypych, Biodegradable composites based on lignocellulosic fibers-an overview, *Prog. Polym. Sci.*, **34** (2009), 982–1021.
6. A. Adamczak-Bugno, G. Świt, A. Krampikowska, Time-frequency analysis of acoustic emission signals generated by cement-fiber boards during bending test, *MATEC Web Conf.*, **174** (2018), 1–10.
7. L. C. Roma, L. S. Martello, H. Savastano, Evaluation of mechanical, physical and thermal performance of cement-based tiles reinforced with vegetable fibers, *Constr. Build. Mater.*, **22** (2008), 668–674.
8. G. Ramakrishna, T. Sundararajan, Studies on the durability of natural fibres and the effect of corroded fibres on the strength of mortar, *Cem. Concr. Compos.*, **27** (2005), 575–582.
9. H. Savastano, P. G. Warden, R. S. P. Coutts, Mechanically pulped sisal as reinforcement in cementitious matrices, *Cem. Concr. Compos.*, **25** (2003), 311–319.
10. K. Schabowicz, T. Gorzelańczyk, M. Szymków, Identification of the degree of degradation of Fibre-cement boards exposed to fire by means of the acoustic emission method and artificial neural networks, *Materials*, **12** (2019), 1–17.
11. R. D. Toledo Filho, F. D. Silva, E. M. R. Fairbairn, J. D. A. M. Filho, Durability of compression molded sisal fiber reinforced mortar laminates, *Constr. Build. Mater.*, **23** (2009), 2409–2420.
12. J. Claramunt, M. Ardanuy, J. A. Garc á-Hortal, R. D. T. Filho, The hornification of vegetable fibers to improve the durability of cement mortar composites. *Cem. Concr. Compos.*, **33** (2011), 586–595.
13. H. Savastano, S. F. Santos, M. Radonjic, W. O. Soboyejo, Fracture and fatigue of natural fiber-reinforced cementitious composites, *Cem. Concr. Compos.*, **31** (2009), 232–243.
14. G. H. D. Tonoli, U. P. Rodrigues Filho, H. Savastano, J. Bras, M. N. Belgacem, F. Rocco Lahr, Cellulose modified fibres in cement based composites, *Compos. Appl. Sci. Manuf.*, **40** (2009), 2046–2053.
15. B. J. Mohr, H. Nanko, K. E. Kurtis, Durability of thermomechanical pulp fiber-cement composites to wet/dry cycling, *Cem. Concr. Res.*, **35** (2005), 1646–1649.
16. K. Schabowicz, Z. Ranachowski, D. Jóźwiak-Niedzwiedzka, L. Radzik, S. Kudela, T. Dvorak, Application of X-ray microtomography to quality assessment of fibre cement boards, *Constr. Build. Mater.*, **110** (2016), 182–188.
17. Z. Z. Ranachowski, D. D. Jóźwiak-Niedźwiedzka, A. M. Brandt, T. T. Dębowski, Application of acoustic emission method to determine critical stress in fibre reinforced mortar beams, *Arch. Acoust.*, **37** (2012), 261–268.
18. K. Schabowicz, J. Hoła, Nondestructive elastic-wave tests of foundation slab in office building, *Mater. Trans.*, **53** (2012), 296–302.
19. J. Hoła, Ł. Sadowski, K. Schabowicz, Nondestructive identification of delaminations in concrete floor toppings with acoustic methods, *Autom. Constr.*, **20** (2011), 799–807.
20. J. Hoła, J. Bień, Ł. Sadowski, K. Schabowicz, Nondestructive and semi-destructive diagnostics of concrete structures in assessment of their durability, *Bull. Polish Acad. Sci. Tech. Sci.*, **63** (2015), 87–96.
21. J. Hola, K. Schabowicz, State-of-the-art nondestructive methods for diagnostics testing of building structures—anticipated development trends, *Arch. Civ. Mech. Eng.*, **11** (2010), 5–11.
22. M. Ardanuy, J. Claramunt, R. D. T. Filho, Cellulosic fiber reinforced cement-based composites: A review of recent research, *Constr. Build. Mat.*, **79** (2015), 115–128.
23. K. Schabowicz, T. Gorzelańczyk, M. Szymków, Identification of the degree of fibre-cement boards degradation under the influence of high temperature, *Autom. Constr.*, **101** (2019), 190–198.

24. G. Świt, Diagnostics of prestressed concrete structures by means of acoustic emission, *IEEE Int. Conf. Reliab.*, **2** (2009), 958–962.
25. G. Świt, Acoustic emission method for locating and identifying active destructive processes in operating facilities, *Appl. Sci.*, **8** (2018), 1–20.
26. B. Goszczyńska, G. Świt, W. Trąmpczyński, Application of the IADP acoustic emission method to automatic control of traffic on reinforced concrete bridges to ensure their safe operation, *Arch. Civ. Mech. Eng.*, **16** (2016), 867–875.
27. B. Goszczyńska, G. Świt, W. Trąmpczyński, Assessment of the technical state of large size steel structures under cyclic load with the acoustic emission method—IADP, *J. Theor. Appl. Mech.*, **52** (2014), 289–299.
28. E. Proverbio, V. Venturi, Reliability of nondestructive tests for on site concrete strength assessment, *10DBMC Int. Conf. Durability Build. Mater. Comp.*, *2*005.
29. B. Goszczyńska, G. Świt, W. Trąmpczyński, Analysis of the microcracking process with the acoustic emission method with respect to the service life of reinforced concrete structures with the example of the RC beams, *Bull. Polish Acad. Sci.: Tech. Sci.*, **63** (2015), 55–65.
30. P. Olaszek, G. Świt, J. R. Casas, On-site assessment of bridges supported by acoustic emission, *Proc. Inst. Civ. Eng. Bridge Eng.*, **169** (2016), 81–92.
31. G. Świt, Evaluation of compliance changes in concrete beams reinforced by glass fiber reinforced plastics using acoustic emission, *J. Mater. Civ. Eng.*, **16** (2004), 414–418.
32. G. Świt, A. Krampikowska, L. Minh Chinh, A prototype system for acoustic emission-based structural health monitoring of my thuan bridge, *Proc. Prognostics Syst. Health Manage. Conf.*, (2016), 624–630.
33. L. Minh Chinh, A. Adamczak, A. Krampikowska, G. Świt, Dragon bridge-the world largest dragon-shaped (ARCH) steel bridge as element of smart city, *E3S Web Conf.*, **10** (2016), 1–5.
34. G. Świt, A. Krampikowska, L. M. Chinh, A. Adamczak, Nhat Tan bridge—the biggest cable-stayed bridge in Vietnam, *Procedia Eng.*, **161** (2016), 666–673.
35. G. Świt, A. Adamczak-Bugno, A. Krampikowska, Bridge management system within the strategic roads as an element of smart city, *IOP Conf. Ser.: Earth Environ. Sci.*, **214** (2019), 1–9.
36. G. Świt, A. Adamczak-Bugno, A. Krampikowska, Application of the acoustic emission method in the assessment of the technical condition of steel structure, *IOP Conf. Ser.: Earth Environ. Sci.*, **214** (2019), 1–10.
37. K. M. Holford, R. J. Lark, Acoustic emission testing of bridges. Inspection and monitoring techniques for bridges and civil structures, *Woodhead Publ. Ltd. CRC*, (2005), 183–215.
38. K. H. Hsieh, M. W. Halling, P. J. Barr, Overview of vibrational structural health monitoring with representative case studies, *J. Bridge Eng.*, **11** (2006), 707–715.
39. H. K. Lee, K. M. Lee, Y. H. Kim, D. B. Bea, Ultrasonic in-situ monitoring of setting process of high performance concrete, *Cem. Concr. Res.*, **34** (2004), 631–640.
40. B. Goszczyńska, G. Świt, W. Trąmpczyński, Monitoring of active destructive processes as a diagnostic tool for the structure technical state evaluation, *Bull. Polish Acad. Sci., Tech. Sci.*, **61** (2013), 97–109.
41. B. Goszczyńska, Analysis of the process of crack initiation and evolution in concrete with acoustic emission testing, *Arch. Civ. Mech. Eng.*, **2** (2014), 134–143.

42. B. Goszczyńska, G. Świt, W. Trąmpczyński, A. Krampikowska, Application of the acoustic emission (AE) method to bridge testing and diagnostics comparison of procedures, *IEEE Prognostics Syst. Health Manage.*, (2012), 1–10.
43. B. Goszczyńska, G. Świt, W. Trąmpczyński, A. Krampikowska, J. Tworzewska, P. Tworzewski, Experimental validation of concrete crack identification and location with acoustic emission method, *Arch. Civ. Mech. Eng.* **12** (2012), 23–28.
44. L. Gołaski, B. Goszczyńska, G. Świt, W. Trąmpczyński, System for the global monitoring and evaluation of damage processes developing within concrete structures under service load, *Balt. J.Road Bridge Eng.*, **7** (2012), 237–245.
45. A. Adamczak-Bugno, G. Świt, A. Krampikowska, Assessment of destruction processes in fiber-cement composites using the acoustic emission method and wavelet analysis, *IOP Conf. Ser.: Mater. Sci. Eng.*, **471** (2019), 1–9.
46. A. Adamczak-Bugno, G. Świt, A. Krampikowska, Scanning electron microscopy in the tests of fibre-cement boards, *MATEC Web Conf.*, **174** (2018), 1–10.

AIMS Press